A&A 507, 833–840 (2009)
DOI: 10.1051/0004-6361/20079144

Astronomy & Astrophysics

The interstellar Ca II distance scale★

A. Megier[1], A. Strobel[1], G. A. Galazutdinov[2], and J. Krełowski[1]

[1] Nicolaus Copernicus University, Center for Astronomy, Gagarina 11, 87-100 Toruń, Poland
e-mail: jacek@astri.uni.torun.pl
[2] Department of Physics and Astronomy, Seoul National University, Gwanak-gu, Seoul 151-747, Korea
e-mail: runizag@gmail.com

Received 26 November 2007 / Accepted 7 July 2009

ABSTRACT

Aims. We attempt to extend the relation between the strengths of the interstellar Ca II lines and the distances to early-type stars to objects beyond 1 kiloparsec, with the line saturation taken into account.

Methods. We measure the Ca II K and Ca II H equivalent widths, and compute Ca II column densities for 262 lines of sight towards early-type stars with available Hipparcos parallaxes (π). The targets are located within a few hundred parsecs of the Galactic plane, and span all the range of Galactic longitudes. We fit the $N_{\rm Ca\,II}$ – parallax relation with a function of the form $\pi = 1/(a \cdot N_{\rm Ca\,II} + b)$, using a maximum-likelihood approach to take account of errors in both variables. We use the resultant formula to estimate distances to stars in OB associations and clusters, and compare them to those found in the literature, usually estimated by spectrophotometric methods.

Results. For lines of sight with $EW(K)/EW(H) > 1.3$, we obtain the following approximate formula for the distance: $D_{\rm Ca\,II} = 77 + (2.78 + \frac{2.60}{\frac{EW(K)}{EW(H)} - 0.932})EW(H)$, where the equivalent widths $EW(K)$ and $EW(H)$ are in mÅ, and the distance $D_{\rm Ca\,II}$ in parsecs. The errors in $D_{\rm Ca\,II}$, resulting from the uncertainty in the fit parameters and errors in the equivalent widths, are typically about 15% of the distance. We can also expect the equation not to hold for objects situated farther than a few hundred parsecs from the Galactic plane. We find several cases of significant column density differences between association or cluster members, especially notable in the Trumpler 16 cluster, indicating either a local contribution to the Ca II column density, or background/foreground stars being confused with members. The ratio $D_{\rm Ca\,II}/D_{\rm assoc}$ appears to depend on the Galactic longitude, being highest in the range $70° < l < 120°$ and lowest for $200° < l < 300°$. This effect may be due to large-scale structure being present in the Ca II layer, or to the nonmember confusion being enhanced in these directions.

Key words. ISM: lines and bands – stars: distances – stars: early-type – open clusters and associations: general

1. Introduction

Estimating distances to stars in our Galaxy, beyond the range of individual trigonometric parallaxes, is a challenging task. The most commonly used method of spectrophotometric parallaxes relies on accurate calibration of the absolute magnitude for the star's spectral type; it is also necessary to take into account interstellar extinction along the line of sight to the star.

The situation is most difficult for early-type stars – typically situated near the Galactic plane, where extinction is highest. Relatively low numbers of stars of any given early subtype make both the classification and calibration of absolute magnitudes for these objects difficult. The differences between M_V values for spectral types O and B, given by different authors (e.g. Schmidt-Kaler 1982; Zorec & Briot 1991; Vacca et al. 1996; Wegner 2006), in some cases (B0III) exceed 1 mag; differences of 0.5 mag. are common. The problem is made more difficult by the fact that the spectral type and luminosity class of any given star is itself uncertain. As the difference of one spectral subclass in OB stars may change the effective temperature by 10 percent or more, any classification uncertainties heavily influence the derived distance. Unresolved binaries, common among early-type stars, may result in distance errors in excess of 40 percent.

It is thus tempting to try to estimate distances assuming as little as possible about the intrinsic parameters of the observed objects, and one of the ways of doing that relies on using the amount of interstellar matter in the line of sight towards the star, calculated on the basis of the star's observed spectrum. The relation of interstellar absorption lines to distance was first studied by Struve (1928). Further work on the subject was published by Sanford (1937), Wilson & Merrill (1937), Evans (1941), and Beals & Oke (1953). Later years saw a lot of research concerning the interstellar absorptions lines, e.g. Welty & Hobbs (2001), Crawford (2001), Price et al. (2001), Crawford et al. (2002), Smoker et al. (2003), Welty et al. (2003), Hunter et al. (2006), Smoker et al. (2006), to name just the more recent ones. However, the possible use of these spectral features for distance estimation was hampered by problems with the calibration of the distance – line strength relation, because of the necessity of finding a substantial sample of appropriately distant stars with well determined distances.

Another problem lies in selecting which of the possible measures of interstellar features should be used for distance estimation, as they correspond to different components of the interstellar medium. The necessary condition is that the given component must be relatively uniformly distributed, at least on the scale of typical distances to the observed stars. While the nonuniform, structure-rich distribution of the interstellar matter is well known, some components are markedly more clumpy than

★ Table 1 is only available in electronic form at http://www.aanda.org

Article published by EDP Sciences

others, resulting in the lower correlation of the associated spectral features with distance. For example, Galazutdinov (2005) and Megier et al. (2005) show that the Ca II is a better distance indicator than K I, Na I or E_{B-V}.

In Megier et al. (2005), the relation between the equivalent widths of the interstellar Ca II lines and the distances of Galactic OB stars was recalibrated with the use of the Hipparcos data. This resulted in formulae for estimating distances, applicable in the range from a few hundred parsecs to slightly over a kiloparsec. In this work, we attempt to extend the range of application of this method to larger distances. This necessitates taking into account the influence of line saturation; thus, we use column densities, instead of equivalent widths.

2. The Ca II observational data

2.1. Spectroscopic observations

Our observational material is listed in Table 1. Most of the spectra were collected during research projects concerning diffuse interstellar bands. The M_V of the targets is between −2.5 and −11, usually between −6 and −10. The signal-to-noise ratio is typically between 50 and 200. The data were aquired during many observing runs between 1999 and 2007 using four Coudé échelle spectrometers:

- The first spectrometer is the MAESTRO[1] fed by the 2-m telescope of the Observatory at Peak Terskol (TE) in the Northern Caucasus (Musaev et al. 1999). The spectrometer is equipped with a Wright Instruments CCD 1242 × 1152 matrix (pixel size 22.5 μm × 22.5 μm) camera. The instrument forms échelle spectra which cover the range from 3500 to 10 100 Å, divided into up to 96 orders. The existing set of gratings and cameras offers several spectral resolutions: from R = 45 000 to 180 000. In this project we used the R = 80 000 as a kind of compromise: it allows us to see discrepancies of the profiles from single gaussians, and also – to observe relatively heavily reddened stars.
- The second spectrometer, covering the Southern hemisphere, is the FEROS[2] spectrograph, fed by the 2.2 m ESO telescope. The resolution of these spectra is constant (R = 48 000). This instrument makes it possible to get the whole available spectral range (~3700−9200 Å, divided into 37 orders) recorded in a single exposure. The flatfielding can be done very precisely in the case of FEROS as it is a fiber-fed spectrograph. We used both the spectra acquired in our two observing runs as well as data taken from the ESO archive.
- Another set of spectra were obtained with the HARPS[3] spectrometer, fed by the 3.6 m ESO telescope in Chile. This spectrograph covers the range ~3800−~6900 Å with the resolution R = 115 000. As an instrument designed to search for exoplanets it guarantees a very precise wavelength calibration.
- The most recent observations were carried out using the fiber-fed echelle spectrograph installed at 1.8-m telescope of the Bohyunsan Optical Astronomy Observatory (BOAO) in South Korea. The spectrograph has three observational modes providing resolving power 30 000, 45 000 and 90 000. In all the cases it allows to record the whole spectral range from ~3500 to ~10 000 Å divided into 75−76 spectral orders. We used the highest resolution mode in our project.

The spectra were reduced using the standard packages: MIDAS[4] and IRAF[5] as well as the DECH[6] code, which provides all standard procedures of image and spectra processing. For this work we selected only stars with spectral types no later than B3; this criterion was used to avoid confusion of the interstellar Ca II lines with possible stellar components. Of the 291 stars in our sample, 267 have Hipparcos parallaxes available.

2.2. Ca II column densities

There are several methods of estimating column densities for partially saturated multicomponent lines. Probably the most accurate method – decomposing the lines into individual velocity components and considering saturation of each of them separately – requires a sample of spectra with very high (and preferably uniform) resolution. The apparent optical depth method (e.g. Savage & Sembach 1991) also requires good spectral resolution. As our aim was to obtain formulae that can be used to estimate distances for relatively faint and distant objects, where spectra of high resolution and quality may be difficult to find, to compute the column densities for the whole sample in a uniform way we used the classical doublet method (e.g. Strömgren 1948). The wavelengths ($\lambda_{\mathrm{Ca\,II K}}$ = 3933.6614 Å and $\lambda_{\mathrm{Ca\,II H}}$ = 3968.4673 Å) and the oscillator strengths ($f_{\mathrm{Ca\,II K}}$ = 0.6346 and $f_{\mathrm{Ca\,II H}}$ = 0.3145) were taken from Morton (2003).

It is well known (see e.g. Nachman & Hobbs 1973) that the doublet method can in some cases produce a significant underestimation of the true column density, especially when the line contains a relatively narrow, heavily saturated component and a wider, partially saturated one. Jenkins (1986) has shown that, for lines containing many components, the straightforward curve-of-growth approach and the doublet method based on it give good results in the majority of cases, as long as the distribution function for various properties of the absorption lines is not too bizarre, enormously saturated lines are absent, and the individual components have curves of growth that saturate in a nearly Gaussian fashion.

To verify the accuracy of our $N_{\mathrm{Ca\,II}}$ estimation, we compared the column densities calculated with the use of the doublet method from our data with those determined by Hunter et al. (2006) from UVES data, using the apparent optical depth method, for the 41 lines of sight that are common to both samples. As can be seen in Fig. 1, the agreement is satisfactory. We can conclude that the doublet method gives sufficiently accurate results in the conditions typical in our sample. While we cannot exclude the possibility that large errors in our estimates of $N_{\mathrm{Ca\,II}}$ could be present, such cases should be rare enough not to bias our conclusions significantly.

The principal sources of measurement errors in the equivalent widths of Ca II are noise in the wavelength interval occupied by the line, and the errors in the placement of the continuum. The former was measured by the spectral reduction packages; the latter is difficult to estimate precisely. The sigmas given in Table 1 were computed under the assumption that the continuum placement results in errors of 5%; this is probably a conservative estimate for stronger lines. The Ca II H line is situated in the wing of the hydrogen $H\epsilon$ line but in high resolution spectra the separation is not difficult.

1 http://www.terskol.com/telescopes/maestro.htm
2 http://www.ls.eso.org/lasilla/sciops/2p2/E2p2M/FEROS
3 http://www.ls.eso.org/lasilla/sciops/3p6/harps

4 MIDAS is distributed by the European Southern Observatory.
5 IRAF is distributed by the National Optical Astronomy Observatories, USA.
6 http://gazinur.com/DECH-software.html

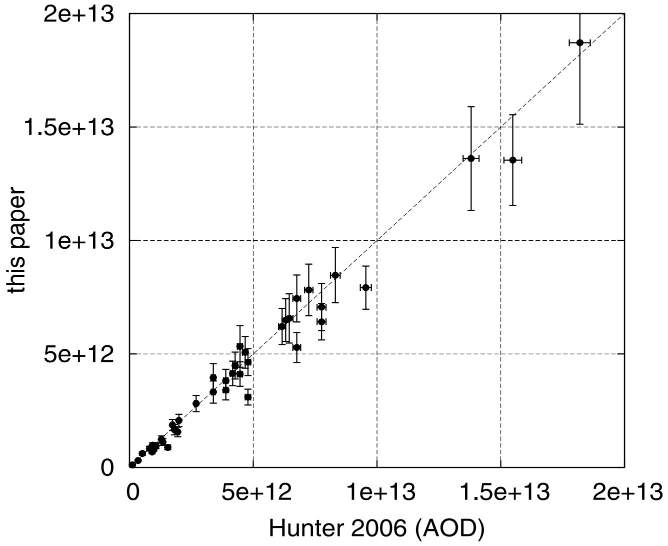

Fig. 1. Ca II column densities obtained in this paper with the doublet ratio method compared to the values computed with the apparent optical depth method by Hunter et al. (2006). The diagonal $y = x$ line is shown for reference.

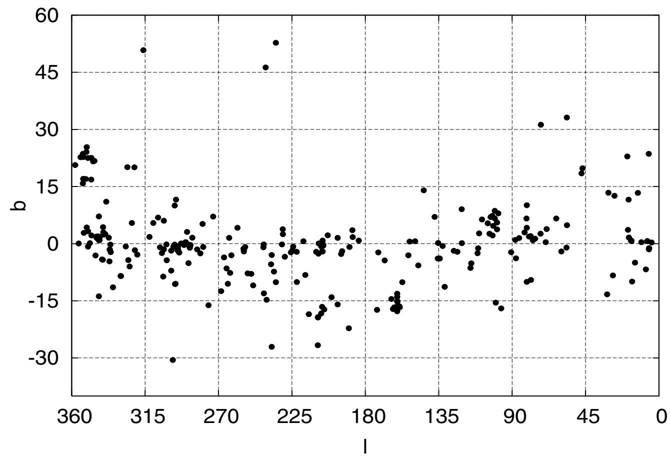

Fig. 2. The distribution of our targets on the sky.

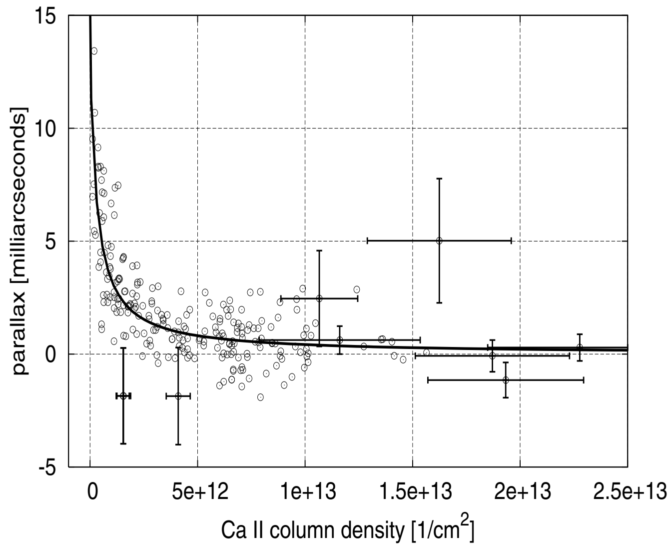

Fig. 3. The column density – parallax relation. For clarity, only the largest errorbars are shown. The maximum likelihood fit is shown with a thick solid line.

3. Parallaxes

The accuracy of the Hipparcos parallaxes (ESA 1997) is typically about 1 miliarcsecond. This makes individual distances derived from these parallaxes very inaccurate beyond a few hundred parsecs. When using the data for such distant objects in a statistical manner, care must be taken to avoid problems that arise because the errors and the measured values are comparable. As the distribution of errors in Hipparcos parallaxes is approximately Gaussian (Arenou & Luri 1999), it is inevitable that for some objects the measured parallax will be negative; it is thus impossible to derive a physically meaningful distance from such values. However, rejection of such objects (or, in general, objects for which σ_π/π is above some threshold) from the sample leads to a statistical bias, as it removes the stars from one wing of the error distribution only. See Smith (2003) for a thorough discussion of the bias and possible corrective procedures. We decided to use parallax values directly, without performing the inversion, and to keep stars with negative parallaxes in the sample.

The errors in the Hipparcos parallaxes may be correlated in objects located close (1°) on the sky; this is the probable cause of the surprisingly large discrepancy between the distance of the Pleiades estimated from the Hipparcos data and from other sources (Munari et al. 2004; Pan et al. 2004; Percival et al. 2005; Soderblom et al. 2005, and references therein). The same effect has been recently reported by Kaltcheva & Makarov (2007) for Collinder 121. As long as there is no systematic, global offset affecting Hipparcos parallaxes, the local correlation of errors should have only limited influence on this work. Our targets are spread in a fairly wide (20°) strip in Galactic latitude and cover all the range of longitudes (see Fig. 2). While some grouping is inevitable as many of the stars are members of OB associations, any significant interval of column densities in Fig. 3 contains stars from different parts of the sky.

4. The Ca II – parallax relation

Of the 267 stars with Hipparcos parallaxes, contained in our sample, 262 were used to find the coefficients of the relation between the $N_{\rm Ca\,II}$ and parallax. The form of the function to fit was similar to that in Megier et al. (2005): $\pi = 1/(a \cdot N_{\rm Ca\,II} + b)$, with the b parameter corresponding to the average size of the Local Bubble. Two stars, HD 66006 and HD 150135, were excluded because of their parallax errors, 6.13 and 8.22 respectively; many times higher than that typical for the Hipparcos data. We also used a threshold of $EW(K)/EW(H) > 1.3$ to exclude heavily saturated cases, where the doublet method is less reliable; this criterion resulted in the exclusion of three other stars: HD 185859, HD 220116, and HD 41997. We have verified however that the elimination of the above five objects has a minimal effect on the fit parameters.

Because of the nonlinear dependence of the column density on the equivalent widths of the doublet lines, the resulting relative errors in $N_{\rm Ca\,II}$ may be significantly larger than those in the equivalent widths themselves. While relative errors in parallax are still generally larger, they are not so dominant as in the case of EW(Ca II H) vs parallax or EW(Ca II K) vs. parallax relations studied in Megier et al. (2005). We thus decided to fit the data using a maximum likelihood algorithm, taking into account errors in both coordinates.

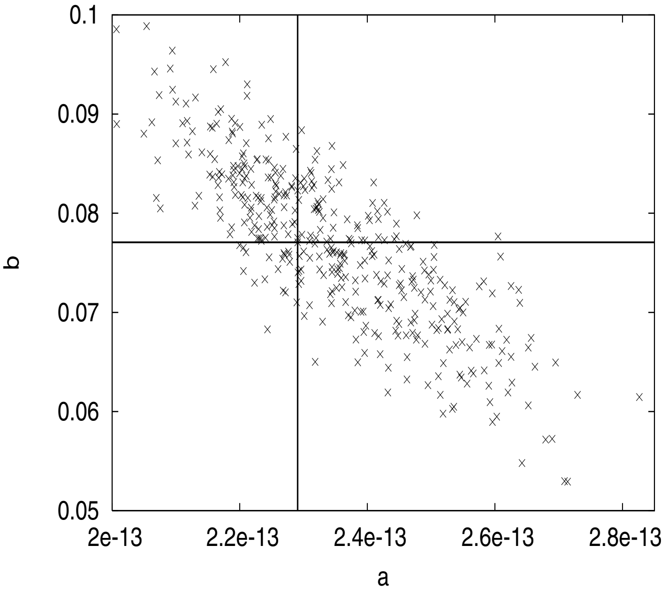

Fig. 4. The distribution of the fit parameters obtained for 400 datasets with added noise. The fit parameter values obtained for the original data are indicated. a is expressed in cm^2/arcsec while b is in 1/arcsec.

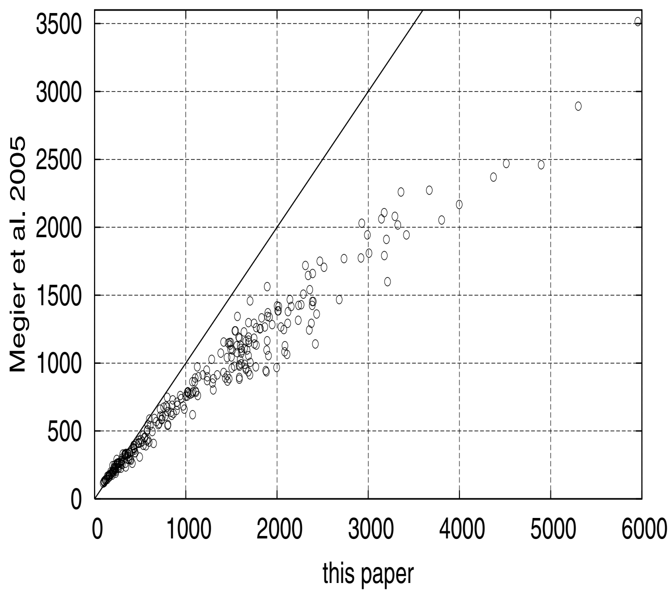

Fig. 5. Distances computed from the equivalent width of the Ca II H line according to Megier et al. (2005), compared to distances obtained from formula (3) in this paper. The $y = x$ diagonal is shown for reference.

The equation of the best-fitting line in Fig. 3 is:

$$\pi = \frac{1}{2.29 \times 10^{-13} \cdot N_{\mathrm{Ca\,II}} + 0.077} \quad (1)$$

where parallax π is in miliarcseconds, and $N_{\mathrm{Ca\,II}}$ in cm^{-2}. The errors in the fit parameters were estimated by running the fitting procedure for 400 artificial datasets generated by adding random gaussian errors to each original data point. The results are presented in Fig. 4. As can be seen, the errors in the fit parameters are correlated; the values are $\sigma_a = 1.56 \times 10^{-14}$, $\sigma_b = 0.0083$, $r_{ab} = -0.83$.

To facilitate the computation of the distance directly from the Ca II equivalent widths, we can approximate the column density, as calculated with the doublet ratio method, by:

$$N_{\mathrm{Ca\,II}} \approx 10^9 \cdot EW(H)\left(12.2 + \frac{11.4}{\frac{EW(K)}{EW(H)} - 0.932}\right), \quad (2)$$

where the equivalent widths are in mÅ, and $N_{\mathrm{Ca\,II}}$ in cm^{-2}. This approximation produces errors of less than 3 percent when $EW(K)/EW(H) > 1.3$. The above formula has no physical justification; it is just the simplest formula that was able to approximate the column density in the desired interval sufficiently well.

Thus, after substituting into (1), the formula for estimating distance is:

$$D_{\mathrm{Ca\,II}} \approx 77 + \left(2.78 + \frac{2.60}{\frac{EW(K)}{EW(H)} - 0.932}\right) EW(H), \quad (3)$$

where the equivalent widths $EW(K)$ and $EW(H)$ are in mÅ, and the distance $D_{\mathrm{Ca\,II}}$ in parsecs.

The errors of distances calculated with the above formula may be correlated for neighbouring stars, as lines of sight towards such objects may well pass through the same interstellar clouds.

Figure 5 presents the comparison of the distances estimated from the equivalent width of the Ca II H line using formula from Megier et al. (2005), and those obtained from formula (3). The differences reach 25 percent at 1000 pc, and 50 percent at 2000 pc. Also notable is the increase in scatter above 1000 pc, probably due to varying level of saturation for stars of the same equivalent width of the Ca II H line. In this paper we calculated column densities taking into account saturations of strong Ca II lines; since they get stronger with distance, the relations by Megier et al. (2005) and the one given in this paper lead to discrepancies at large distances. The formula (1) should give reasonable distance estimates up to 3 kpc in the Galactic plane. The current size of our sample of objects does not allow to involve into the formula terms describing any dependence on the Galactic latitude.

5. Comparison with association distances

As evident from Fig. 3, the majority of the stars on which the Ca II distance calibration is based, are located at distances of several hundred parsecs, corresponding to parallaxes ≥1 milliarcsecond. To check whether the formula (3) can be successfully used for larger distances, we would need a significant sample of early-type stars (so that the interstellar Ca II can be accurately measured), with well determined distances from some independent source. At distances ≥1 kpc, most of the stars bright enough to allow us to measure the Ca II lines in reasonable observation time with telescopes of moderate size are either very early-type (O7 and earlier) or supergiants; for such objects the absolute magnitude calibration is particularly uncertain.

We may however expect that the distances to OB associations and clusters, found in the literature, should be somewhat more accurate that those of individual early-type stars. Although they are usually, with the exception of the closest associations, dependent on luminosity calibration of early-type stars, they are based on a number of measurements for stars of different spectral types, and so should be less prone to errors resulting from the poorly known properties of stars of any specific spectral type or luminosity class.

The use of such distances poses another problem however: uncertain association membership of any given star. Many studies of Galactic OB associations have revealed that they can't be

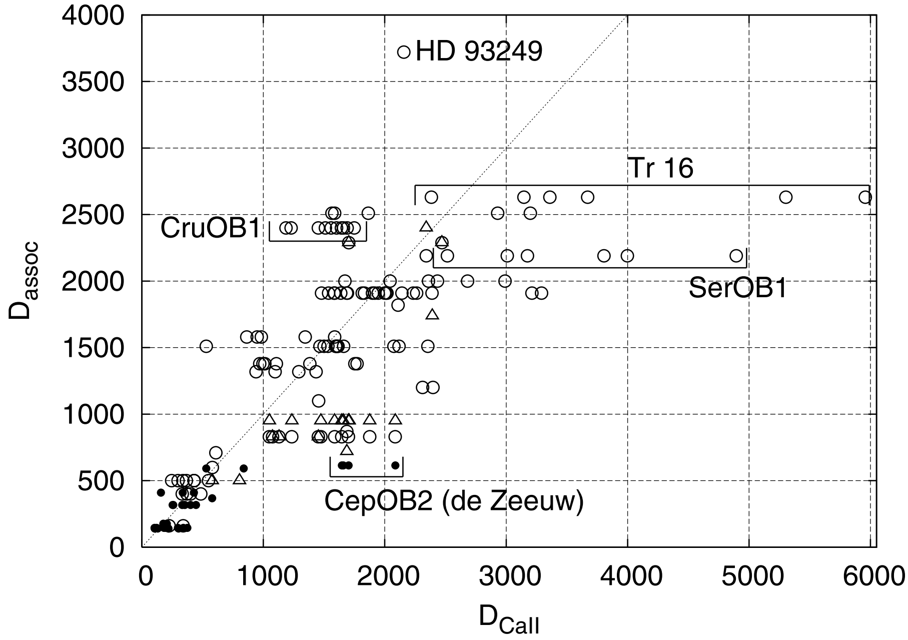

Fig. 6. Distances estimated from the Ca II lines (abscissa) versus distances from association membership from different sources (ordinate). Symbols: open circles – Humphreys (1978); open triangles – Garmany & Stencel (1992); full circles – de Zeeuw et al. (1999). Objects discussed in the text are indicated.

treated as spatially isolated, monolithic structures. The presence of substructures of different evolutionary ages is common. The definition of the borders and membership of the given association is often problematic. Irregular shape and nonuniform distribution of stars often make the delimitation of the association a matter of the researchers choice (Garmany 1994). The situation is made more complicated by selection effects resulting from the interstellar extinction, and the effects of projection on the sky: an elongated volume with enhanced, but not uniform, OB star density, seen along its length, is likely to be regarded as one association; the same structure seen from the perpendicular direction may be broken into several smaller associations.

We did not try to define our own criteria for the association membership, relying predominantly on the members lists and distances given by Humphreys (1978) and Garmany & Stencel (1992). We have also included the data for the nearby (≤1 kpc) association from de Zeeuw et al. (1999).

As can be seen in Fig. 6, the relation between stellar distances estimated from the Ca II lines and those ascribed on the basis of association/cluster membership is far from perfect. There is no obvious systematic bias, however, the scatter is large; the ratio $D_{\text{Ca II}}/D_{\text{assoc}}$ may vary from below 0.5 to over 2.0. Below we discuss the most conspicuous cases of discrepancy.

The large difference between the Ca II distance and that given by de Zeeuw et al. (1999) for the Cep OB2 association (based on averaged Hipparcos parallaxes) may be partially due to a systematic bias resulting from selecting only stars with positive parallaxes; while a correction for this bias was applied by de Zeeuw et al. (1999), the value of the correction depends on the parallax errors and the shape and size of the association. Kaltcheva & Makarov (2007) show that, despite the correction, the combined effect of the correlated parallax errors and the bias resulting from the removal of the negative parallaxes can be significant (about 35 percent in the case of Collinder 121).

A very interesting case is that of the Trumpler 16 stars in the Carina complex. The distance to Trumpler 16 is usually estimated as about 2.5 kpc (e.g. Walborn 1995); however, Carraro et al. (2004) estimate it to be 4 kpc. The Ca II lines in the five objects in our sample that are regarded as members of this cluster (HD 93250, HD 303308, CD-59 3300, CD-59 3303 and HD 93403) vary from $EW(K) = 414$ mÅ (HD 93403) to 841 mÅ for HD 93250 and 1074 mÅ in the case of HD 303308. The corresponding range of distances estimated from formula (3) is 2400−5800 pc. The M_{bol} of HD 93250 and HD 303308 are given by Sanchawala et al. (2007) as −11.3 and −10.4 respectively, at the distance of 2500 pc. Increasing the distances to 5200 and 5800 pc, as suggested by the intensities of the Ca II lines, would make these stars as luminous as $M_{\text{bol}} = -12.9$ and −12.2 respectively, making them the most luminous stars known in our Galaxy. Such a concentration of superluminous stars at different distances in a small region of the sky seems extremely unlikely; the only apparent explanation of such a structure would be a huge front of massive star formation, seen along its length. The more probable hypothesis is that the local contributions to the column density of the Ca II are responsible, possibly related to the nearby η Carinae (about 1′ away from HD 303308, and 8′ away from HD 93250). However, the very complex profiles of the ionized Ca lines, seen in this object, are very likely due to circumstellar envelopes since profiles of diffuse interstellar bands do not show any sign of the Doppler splitting. They look like they originated in a single cloud.

The Ca II lines of the five stars in the Trumpler 16 cluster are shown in Fig. 7. It is evident that the velocity structure of the material is complex. However, the main velocity component seen in HD 93403 is present in all other cases; if we interpret all the other components as originating in material local to the cluster, the distance to Trumpler 16 would be that of the HD 93403 (2360 pc), in good agreement with the majority of the spectrophotometric estimates.

The distance to the Cru OB1 association in Humphreys (1978) is 2400 pc; Kaltcheva & Georgiev (1994) estimate it to be 2730 pc. The interstellar Ca II lines seen in the spectra of 10 stars in this association that are in our sample are shown in Fig. 8. All the spectra show two main radial velocity components, but their relative strength varies. The average distance to this association, estimated from formula (3), is 1510 pc, with the individual values ranging from 1180 pc for HD 101190 to 1730 pc for HD 100099.

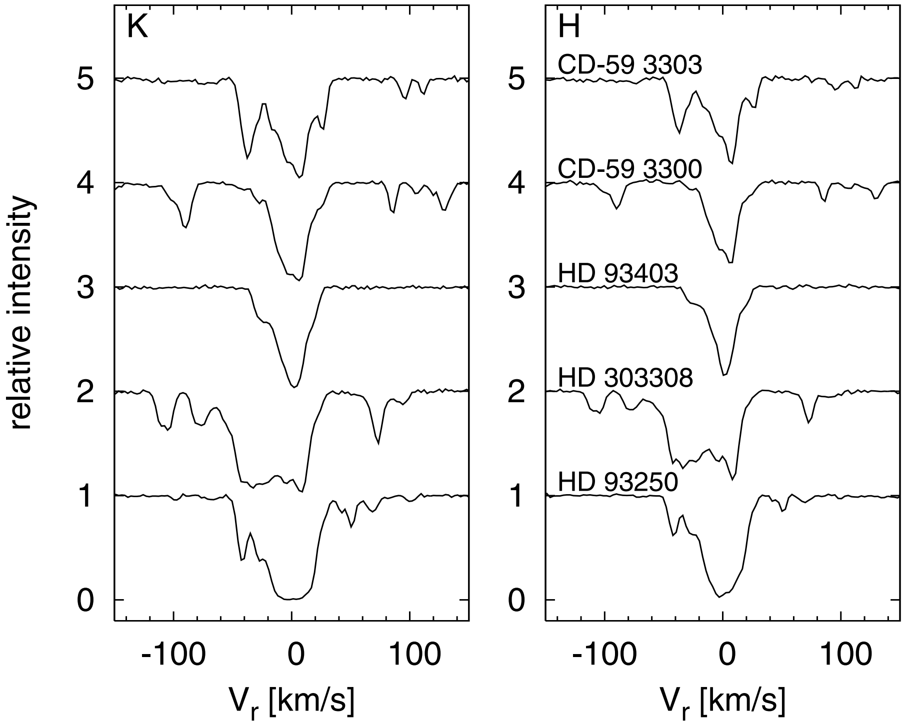

Fig. 7. The Ca II lines in the Tr16 cluster. The order of the stars is the same in both panels.

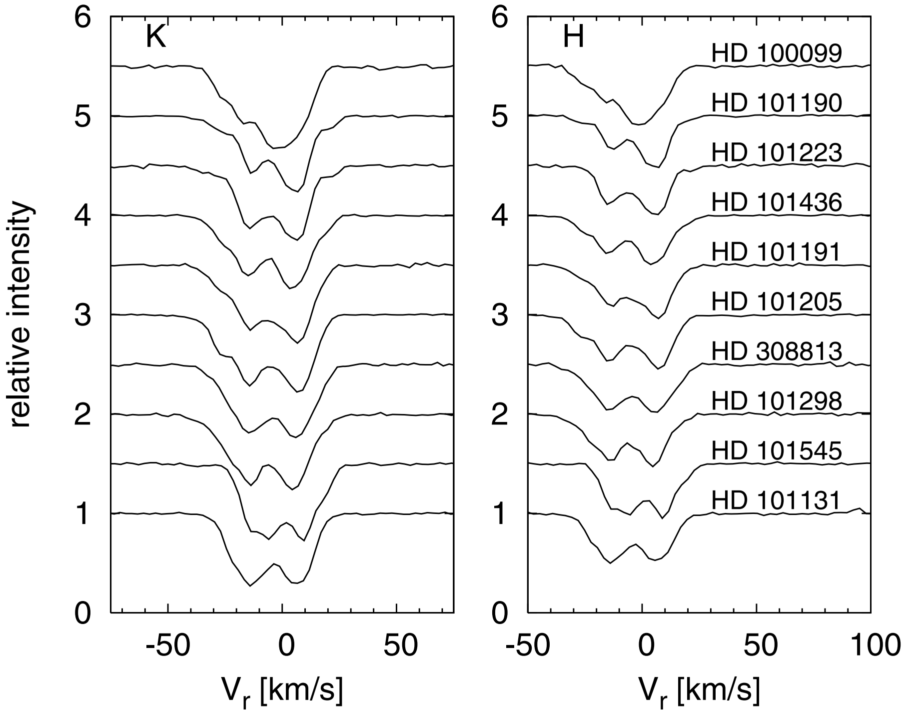

Fig. 8. The Ca II lines in the Cru OB1 association.

The distance to the Ser OB1 association in Humphreys (1978) is 2190 pc. As evident from Fig. 6, the distances to the individual stars estimated from Ca II vary in a fairly wide interval from 2480 to over 4850 pc. All the Ser OB1 stars in our sample are members of the cluster NGC 6611, rich in massive, early type stars. The minimum of the Ca II distances to objects in this association is in reasonably good agreement with the value given by Humphreys (1978). It would seem natural to attribute the spread in Ca II distances to additional radial velocity components due to matter related to the cluster, the situation being similar to that in Trumpler 16. However, Fig. 9 shows that, at least at the spectral resolution R = 48 000, we cannot separate any set of velocity components common to all the stars, which we could reliably attribute to “truly interstellar” matter in front of the cluster, and thus expect to be a reasonably good measure of the clusters distance. Note e.g. the striking differences between the Ca II profiles seen towards BD-13 4927 and BD-13 4929, situated about 3′ apart on the sky.

HD 93249 (top of Fig. 6) is listed by Humphreys (1978) as a member of Trumpler 15, at the distance of 3720 pc. The more recent value given by Carraro (2002) is 2400 pc, in good agreement with our estimate.

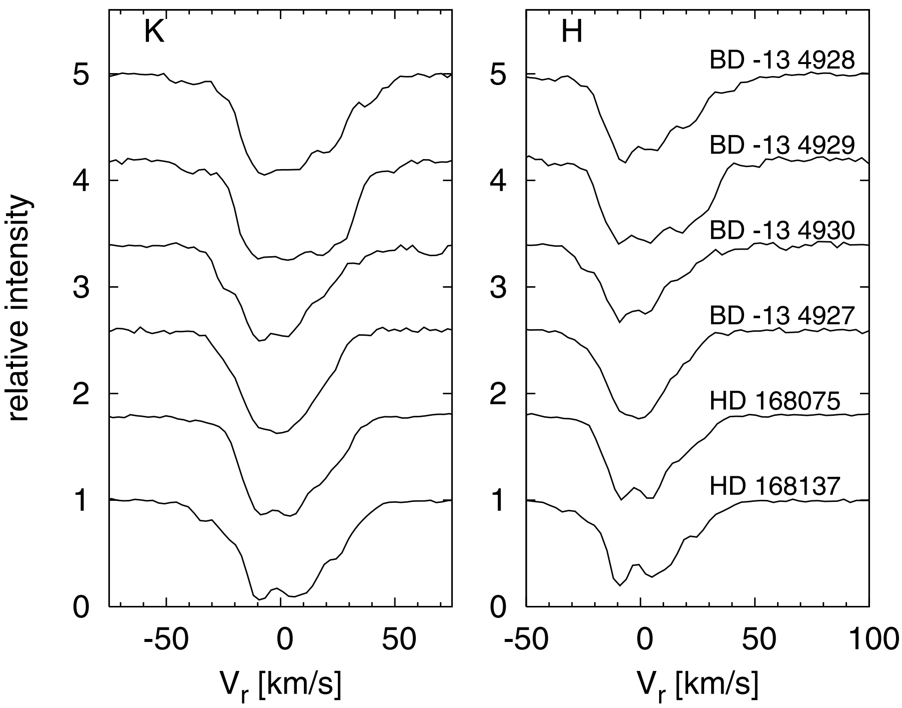

Fig. 9. The Ca II lines in the Ser OB1 association. The spectra were adjusted in radial velocity so that the dominant components of the interstellar CH lines correspond.

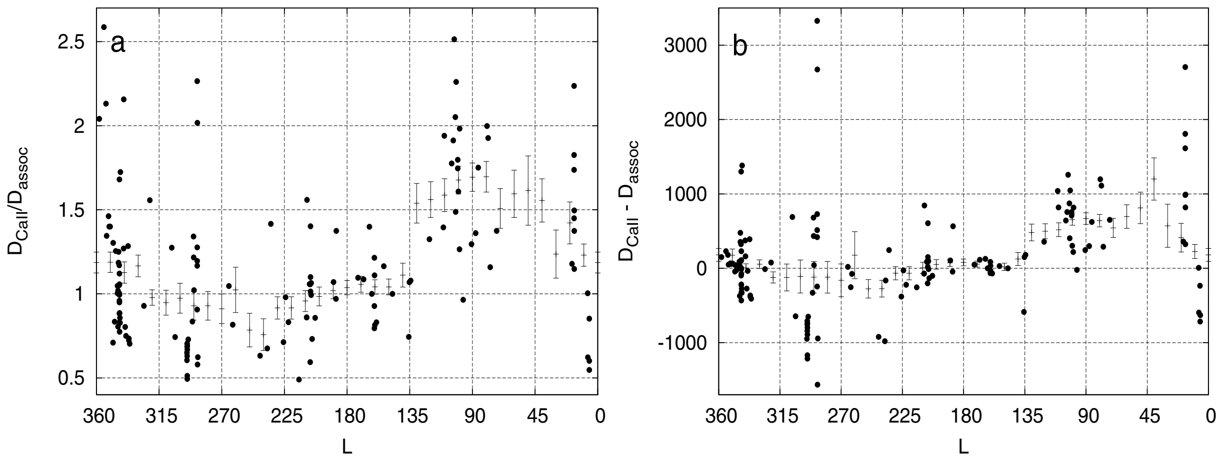

Fig. 10. The ratio $D_{\mathrm{Ca\,II}}/D_{\mathrm{assoc}}$ **a)** and the difference $D_{\mathrm{Ca\,II}} - D_{\mathrm{assoc}}$ **b)** as a function of Galactic longitude. The running average in 60° bins at 10° intervals is also shown, with 1 sigma errors.

Figure 10a presents the dependence of $D_{\mathrm{Ca\,II}}/D_{\mathrm{assoc}}$ on galactic longitude. While scatter is conspicuous, there is apparently some systematic effect: the ratio tends to be lower between $200 < l < 300$ and higher in the region $50 < l < 120$. The tendency is also visible in Fig. 10b showing the $D_{\mathrm{Ca\,II}} - D_{\mathrm{assoc}}$ as a function of galactic longitude. One of the possible reasons for this effect is the presence of large scale structure in the Ca II layer. This would undermine the utility of the Ca II lines for distance determination, unless the effect is taken into account in the formula (3). Another possibility is the inclusion of background or foreground stars in the associations. Such a situation is more likely in regions where the density of early-type objects on the sky is higher – towards the Galactic center, or along the direction of a spiral arm.

Figures 11a and b show the ratio $D_{\mathrm{Ca\,II}}/D_{\mathrm{assoc}}$ and the difference $D_{\mathrm{Ca\,II}} - D_{\mathrm{assoc}}$ as a function of galactic latitude. While Fig. 11a might suggest some systematic effect, as the value of $D_{\mathrm{Ca\,II}}/D_{\mathrm{assoc}}$ is higher for positive b, Fig. 11b shows that the actual differences in distance are small. The few stars located at higher latitudes are relatively nearby, and the differences are probably due to local inhomogeneities in the Ca II structure.

The scale height of the Ca II layer in our Galaxy is estimated to be ≈800 pc (Smoker et al. 2003). For objects located at $|z|$ close to or greater than that value, we can expect the formula (3) to systematically underestimate the true distance. However, it should be possible to detect such cases; the value of $|z|$ computed from such an underestimated distance would be close to 800 pc. In our sample of stars the the values of $|z|$ estimated from the Ca II distances do not exceed 450 pc, and in all except four stars fall below 300 pc.

6. Conclusions

The Ca II lines apparently can provide information related to the distance of early-type stars beyond the current range of trigonometric parallaxes, but the accuracy and reliability of the method is limited. The possible local enhancements in the Ca II column density, related to the given star or its parent cluster/association,

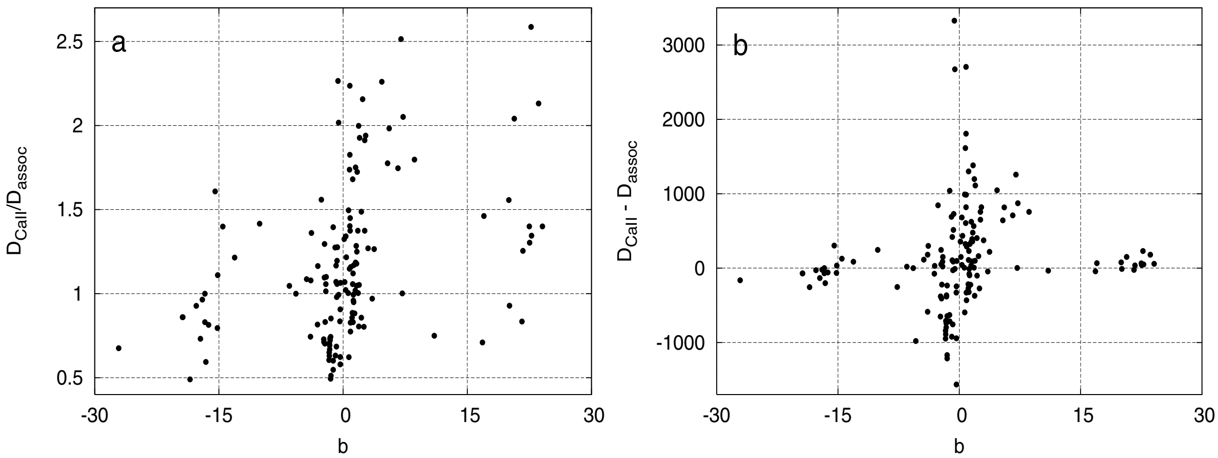

Fig. 11. The ratio $D_{\rm Ca\,II}/D_{\rm assoc}$ **a)** and the difference $D_{\rm Ca\,II} - D_{\rm assoc}$ **b)** as a function of Galactic latitude.

can lead to large errors in individual cases; while such local effects could probably be detected if very high resolution spectra of the star and its neighbours were available, their contribution might be difficult to estimate, especially in cases where saturation is significant. The possible large-scale structure in the Ca II layer, suggested by Figs. 10a and b, can also affect the accuracy of the distance determination. While such a structure, if confirmed, would merit a closer look itself, our present dataset is not sufficient to study it in any detail.

It is possible that combining (e.g. in a Bayesian framework) the distance information obtained from Ca II lines with other data, like Ti II lines, trigonometric, or spectroscopic parallaxes, could result in more accurate distance determinations. Future astrometric missions will provide a set of parallax measurements which, for their target stars, will supersede any distance estimates based on interstellar lines. They may also allow a refinement of the relation between interstellar line strength and distance, making it possible to estimate distances for the objects whose trigonometric parallaxes will not be measured.

Acknowledgements. The authors acknowledge the financial support of the Polish State during the period 2007−2010 (grant N203 012 32/1550). We are deeply grateful to the ESO archive as well as to the ESO staff members who assisted us while conducting our own observing runs.

References

Arenou, F., & Luri, X. 1999, ASP Conf. Ser., 167, 13
Beals, C. S., & Oke, J. B. 1953, MNRAS, 113, 530
Carraro, G. 2002, MNRAS, 331, 785
Carraro, G., Romaniello, M., Ventura, P., & Patat, F. 2004, A&A, 418, 525
Crawford, I. A. 2001, MNRAS, 328, 1115
Crawford, I. A., Lallement, R., Price, R. J., et al. 2002, MNRAS, 337, 720
ESA 1997, The Hipparcos and Tycho Catalogues, ESA SP-1200 (Noordwijk: ESA)
Evans, J. W. 1941, ApJ, 93, 275
Galazutdinov, G. A. 2005, JKAS, 38, 215
Garmany, C. D. 1994, PASP, 106, 25
Garmany, C. D., & Stencel, R. E. 1992, A&AS, 94, 211
Humphreys, R. M. 1978, ApJSS, 38, 309
Hunter, I., Smoker, J. V., Keenan, F. P., et al. 2006, MNRAS, 367, 1478
Jenkins, E. B. 1986, ApJ, 304, 739
Kaltcheva, N. T., & Georgiev, L. N. 1994, MNRAS, 269, 289
Kaltcheva, N., & Makarov, V. 2007, ApJ, 667, L155
Megier, A., Strobel, A., Bondar, A., et al. 2005, ApJ, 634, 451
Morton, D. C. 2003, ApJS, 149, 205
Munari, U., Dallaporta, S., Siviero, A., et al. 2004, A&A, 418, L31
Musaev, F. A., Galazutdinov, G. A., Sergeev, A. V., et al. 1999, Kinematics Phys. Celest. Bodies, 15, 216
Nachman, P., & Hobbs, L. M. 1973, ApJ, 182, 481
Pan, X., Shao, M., & Kulkarni, S. R. 2004, Nature, 427, 326
Percival, S. M., Salaris, M., & Groenewegen, M. A. T. 2005, A&A, 429, 887
Price, R. J., Crawford, I. A., Barlow, M. J., & Howarth, I. D. 2001, MNRAS, 328, 555
Sanchawala, K., Chen, W. P., Lee, H. T., et al. 2007, ApJ, 656, 462
Sanford, R. F. 1937, ApJ, 86, 136
Savage, B. D., & Sembach, K. R. 1991, ApJ, 379, 245
Schmidt-Kaler, T. 1982, in Landolt-Börnstein New Series, Group VI, Volume 2b, ed. K. Schaifers, & H. H. Voigt (Berlin: Springer)
Smith, H. 2003, MNRAS, 338, 891
Smoker, J. V., Rolleston, W. R. J., Kay, H. R. M., et al. 2003, MNRAS, 346, 119
Smoker, J. V., Lynn, B. B., Christian, D. J., & Keenan, F. P. 2006, MNRAS, 370, 151
Soderblom, D. R., Nelan, E., Benedict, G. F., et al. 2005, AJ, 129, 1616
Strömgren, B. 1948, ApJ, 108, 242
Struve, O. 1928, ApJ, 67, 353
Vacca, W. D., Garmany, C. D., & Shull, J. M. 1996, ApJ, 460, 914
Walborn, N. R. 1995, Rev. Mex. Astron. Astrofis., 2, 51
Wegner, W. 2006, MNRAS, 371, 185
Welty, D. E., & Hobbs, L. M. 2001, ApJS, 133, 345
Welty, D. E., Hobbs, L. M., & Morton, D. C. 2003, ApJS, 147, 61
Wilson, O. C., & Merrill, P. W. 1937, ApJ, 86, 44
de Zeeuw, P. T., Hoogerwerf, R., de Bruijne, J. H. J, Brown, A. G. A., & Blaauw, A. 1999, AJ, 117, 354
Zorec, J., & Briot, D. 1991, A&A, 245, 150

Table 1. Target stars. Columns: name – star name; l, b – Galactic coordinates (from SIMBAD); π, σ_π – trigonometric parallax and its error (Hipparcos); K, σ_K – the equivalent width of the Ca II K line and its error; H, σ_H – the equivalent width of the Ca II H line and its error; $N_{Ca\,II}$, $\sigma_{N_{Ca\,II}}$ – Ca II column density and its error; as, as ref: association membership and reference: H stands for Humphreys (1978), GS for Garmany and Stencel (1992), Z for de Zeeuw et al. (1999). D_H – association distance (in parsecs) from Humphreys (1978); D_{GS} – association distance from Garmany & Stencel (1992); D_Z – association membership and distance from de Zeeuw et al. (1999); $D_{Ca\,II}$, $\sigma_{D_{Ca\,II}}$ – distance estimated from formula (3), and its formal error.

Name	l	b	π	σ_π	K	σ_K	H	σ_H	$N_{Ca\,II}$	$\sigma_{N_{Ca\,II}}$	as	as ref	D_H	D_{GS}	D_Z	$D_{Ca\,II}$	$\sigma_{D_{Ca\,II}}$
		mÅ		mÅ	10^{12} cm^{-2}				pc	pc	pc	pc	pc				
BD-13 4928	016.9670	+00.8242	...	...	619	32	451	26	17.1	3.61	SerOB1	H	2190	...	...	3998	866
BD-13 4929	016.9776	+00.8159	...	...	684	36	515	27	21.0	4.53	SerOB1	H	2190	...	...	4896	1086
BD-13 4927	016.9843	+00.8459	...	...	515	28	369	20	13.5	2.66	SerOB1	H	2190	...	...	3176	643
BD-13 4930	016.9437	+00.7664	2.46	2.12	544	30	350	21	10.6	1.82	SerOB1	H	2190	...	...	2515	447
CD-59 3300	287.6021	–00.7375	...	...	653	35	428	23	13.4	2.17	Tr16	H	2630	...	...	3145	536
CD-59 3303	287.5885	–00.6870	...	...	732	40	471	25	14.3	2.24	Tr16	H	2630	...	...	3359	556
HD 2083	120.9137	+09.0357	1.07	0.56	239	18	125	14	2.97	0.68	...	...	...	...	...	757	161
HD 2905	120.8361	+00.1351	0.79	0.52	235	13	167	10	6.02	1.25	CasOB14	H	1100	...	...	1457	300
HD 5394	123.5769	–02.1484	5.32	0.80	17	2.1	8	1.1	0.17	0.05	...	...	...	...	...	117	12
HD 7252	125.6820	–01.8678	2.30	0.78	284	20	214	20	8.76	3.11	...	...	...	...	...	2083	725
HD 10516	131.3247	–11.3301	4.50	0.73	24	1.6	16	1.5	0.51	0.14	Cas-Tau	Z	...	...	...	195	32
HD 13256	132.5985	–00.6435	-0.08	1.17	608	32	418	23	14.2	2.55	...	...	...	...	...	3323	622
HD 13854	134.3814	–03.9054	1.37	0.70	578	30	360	19	10.5	1.52	PerOB1	H, GS	2290	2290	...	2470	381
HD 14818	135.6167	–03.9333	0.92	0.66	560	30	296	16	7.10	0.84	PerOB1	H, GS	2290	2290	...	1704	219
HD 15785	135.3058	+00.1877	2.90	1.05	537	28	337	19	9.88	1.53	CasOB6	H, GS	2190	2400	...	2341	380
HD 20336	137.4570	+07.0610	4.07	0.62	32	2.1	18	2	0.46	0.11	Cas-Tau	Z	...	...	...	183	26
HD 21428	147.4461	–05.6961	5.84	0.85	47	3.2	21	1.8	0.44	0.07	alphaPer	Z	...	...	177	177	16
HD 22951	158.9199	–16.7030	3.53	0.88	103	5.3	50	2.7	1.11	0.12	PerOB2	H, Z	400	...	318	332	30
HD 23060	158.9916	–16.4519	2.09	0.93	92	6.2	63	6.7	2.12	0.67	...	...	...	...	...	563	157
HD 23180	160.3637	–17.7399	2.21	0.84	76	3.9	46	2.5	1.28	0.18	PerOB2	H	400	...	...	371	44
HD 23625	160.0806	–16.2551	2.63	1.00	66	5	34	4.5	0.80	0.21	PerOB2	Z	...	...	318	259	49
HD 24131	160.2266	–15.1369	3.15	0.84	68	4.2	42	3.5	1.20	0.26	PerOB2	Z	...	...	318	353	60
HD 24190	160.3875	–15.1837	2.04	1.00	73	5.5	35	3.8	0.77	0.16	PerOB2	Z	...	...	318	253	37
HD 24398	162.2891	–16.6904	3.32	0.75	57	2.9	40	2.3	1.41	0.27	PerOB2	H, Z	400	...	318	400	64
HD 24534	163.0814	–17.1362	1.21	0.94	142	7.8	96	5.5	3.16	0.57	...	...	...	...	...	801	138
HD 24640	160.4687	–13.9738	3.36	0.76	91	5.9	52	3.6	1.35	0.22	...	...	...	...	...	387	54
HD 24760	157.3538	–10.0885	6.06	0.82	34	2.7	22	3.5	0.67	0.28	...	...	...	...	...	232	65
HD 24912	160.3723	–13.1065	1.84	0.70	115	5.9	67	3.5	1.78	0.23	PerOB2	H	400	...	...	486	57
HD 25348	149.3844	+00.6689	–0.71	0.97	248	18	182	18	7.02	2.46	...	...	...	...	...	1684	573
HD 25799	163.9577	–14.5242	2.78	0.95	80	4.8	52	4.6	1.61	0.39	PerOB2	Z	...	...	318	445	91
HD 25940	153.6542	–03.0451	5.89	0.72	39	2	22	1.2	0.56	0.07	alphaPer	Z	...	...	177	206	17
HD 27192	152.8033	+00.5738	2.74	0.75	95	6	48	3.3	1.10	0.16	...	...	...	...	...	330	38
HD 27778	172.7629	–17.3928	4.49	1.11	52	6.6	28	4.9	0.68	0.26	...	...	...	...	...	234	59
HD 29138	297.9870	–30.5423	0.37	0.54	199	10	111	5.8	2.81	0.34	...	...	...	...	...	722	87
HD 30614	144.0656	+14.0424	0.47	0.60	282	14	195	9.8	6.68	1.12	...	...	...	...	...	1607	275
HD 30677	190.1808	–22.2169	1.97	0.91	299	15	174	8.8	4.63	0.58	...	...	...	...	...	1137	148
HD 31327	168.1414	–04.4022	0.28	0.86	248	14	172	9.3	5.92	1.09	AurOB1	H	1320	...	...	1434	265
HD 33328	209.1402	–26.6856	1.86	0.88	95	4.8	51	2.6	1.24	0.14	...	...	...	...	...	362	35
HD 34078	172.0813	–02.2592	2.24	0.74	132	6.9	77	4.2	2.05	0.28	OriOB1	H	500	...	...	548	68
HD 35468	196.9278	–15.9532	13.42	0.98	15	0.81	8	0.57	0.19	0.03	...	...	...	...	...	121	9
HD 37022	209.0108	–19.3841	–1.85	2.12	103	6.2	59	4.7	1.54	0.28	OriOB1	H	500	...	...	430	67
HD 37023	209.0103	–19.3804	–1.85	2.12	117	8.9	63	6.1	1.54	0.32	OriOB1	H	500	...	...	430	76

Table 1. continued.

Name	l	b	π	σ_π	K	σ_K	H	σ_H	$N_{Ca II}$	$\sigma_{N_{Ca II}}$	as	as ref	D_H	D_{GS}	D_Z	$D_{Ca II}$	$\sigma_{D_{Ca II}}$
		mÅ		mÅ	10^{12} cm^{-2}				pc	pc	pc	pc	pc				
HD 37055	207.0417	–18.3349	1.25	0.92	117	6	50	2.7	1.01	0.10	...	...	...	...	...	309	24
HD 37061	208.9248	–19.2736	2.77	0.88	80	5.2	52	4.7	1.61	0.40	...	...	...	...	...	445	94
HD 37128	205.2121	–17.2417	2.43	0.91	90	6.2	50	5.4	1.26	0.30	OriOB1	H	500	...	...	366	70
HD 37490	200.7341	–14.0322	2.01	0.94	128	6.5	76	3.9	2.07	0.27	...	...	...	...	...	552	67
HD 37742	206.4523	–16.5852	3.99	0.79	88	7	43	4.4	0.96	0.19	OriOB1	H	500	...	...	297	45
HD 38666	237.2862	–27.1021	2.52	0.55	96	4.8	49	2.5	1.14	0.12	OriOB1	H	500	...	...	338	30
HD 38771	214.5143	–18.4965	4.52	0.77	78	7.2	35	4.6	0.73	0.17	OriOB1	H	500	...	...	245	40
HD 40111	183.9655	+00.8388	1.55	0.84	164	8.4	99	5.1	2.76	0.37	...	...	...	...	...	708	93
HD 41117	189.6918	–00.8604	0.10	0.89	331	17	216	11	6.71	1.02	GemOB1	H	1510	...	...	1615	254
HD 41753	194.8064	–02.7212	6.10	0.88	34	2.1	14	1.1	0.28	0.04	Cas-Tau	Z	...	...	...	140	10
HD 41997	194.1450	–01.9811	1.10	1.18	290	15	227	12	10.2	2.46	...	...	...	...	...	2420	584
HD 42087	187.7518	+01.7688	–0.51	1.15	358	20	250	14	8.72	1.67	GemOB1	H	1510	...	...	2075	404
HD 43384	187.9942	+03.5287	1.56	0.87	392	30	228	16	6.06	1.08	GemOB1	H	1510	...	...	1465	263
HD 45314	196.9593	+01.5246	2.19	1.04	277	14	188	9.9	6.23	1.05	...	...	...	...	...	1504	256
HD 45725	216.6614	–08.2139	4.72	1.10	29	1.5	14	0.76	0.31	0.03	...	...	...	...	...	148	9
HD 46149	206.2200	–02.0389	–0.15	1.23	262	13	188	9.8	6.91	1.29	MonOB2	H	1510	...	...	1661	313
HD 46150	206.3058	–02.0695	1.97	0.88	281	14	191	9.7	6.35	1.04	MonOB2	H	1510	...	...	1531	255
HD 46185	221.9706	–10.0784	2.22	0.87	114	5.7	68	3.4	1.86	0.24	...	...	...	...	...	504	60
HD 46223	206.4382	–02.0737	0.57	0.95	297	15	201	10	6.63	1.06	MonOB2	H	1510	...	...	1596	262
HD 46573	208.7297	–02.6311	0.83	1.11	334	17	249	13	9.94	2.06	MonOB2	H	1510	...	...	2354	494
HD 46966	205.8096	–00.5491	–1.22	0.96	322	16	206	11	6.21	0.94	MonOB2	H	1510	...	...	1500	234
HD 47129	205.8740	–00.3111	–0.74	0.80	322	16	212	11	6.68	1.04	MonOB2	H	1510	...	...	1608	258
HD 47240	206.9758	–00.7466	–0.68	0.79	357	18	225	12	6.64	0.98	MonOB2	H	1510	...	...	1598	245
HD 47432	210.0349	–02.1105	0.96	0.89	271	14	181	9.1	5.84	0.92	...	...	...	...	...	1414	228
HD 47839	202.9363	+02.1985	3.19	0.73	180	9.4	96	5.5	2.32	0.29	MonOB1	H	710	...	...	609	73
HD 48099	206.2096	+00.7982	–0.08	0.77	376	19	260	13	8.91	1.50	MonOB2	H	1510	...	...	2117	367
HD 48434	208.5443	+00.0621	–0.14	0.76	209	11	128	6.5	3.63	0.50	...	...	...	...	...	909	125
HD 49131	240.5001	–14.7267	2.06	0.90	74	3.7	36	1.8	0.80	0.08	...	...	...	...	...	261	20
HD 50896	234.7568	–10.0832	1.74	0.76	191	10	117	6.5	3.32	0.49	Coll121	Z	...	...	592	838	121
HD 51411	242.2075	–13.0292	2.30	0.58	27	1.4	19	1.1	0.67	0.13	...	...	...	...	...	231	31
HD 52382	222.1707	–02.1549	1.11	0.79	283	14	166	8.6	4.46	0.58	CMaOB1	H	1320	...	...	1098	146
HD 52918	218.0123	+00.6139	2.92	0.87	68	3.5	32	1.7	0.69	0.07	...	...	...	...	...	236	17
HD 53974	224.7096	–01.7938	1.15	0.92	189	9.6	120	6.2	3.58	0.52	...	...	...	...	...	897	130
HD 53975	225.6786	–02.3157	0.66	0.77	251	13	144	7.5	3.77	0.48	CMaOB1	H	1320	...	...	940	121
HD 54309	236.0061	–07.3390	1.10	0.74	38	2.1	21	1.3	0.53	0.07	...	...	...	...	...	198	18
HD 54662	224.1685	–00.7784	0.56	0.81	245	12	164	8.3	5.31	0.84	CMaOB1	H	1320	...	...	1293	206
HD 54764	229.4250	–03.4396	–0.09	0.68	141	7.2	86	4.5	2.43	0.34	...	...	...	...	...	633	83
HD 57060	237.8244	–05.3679	1.09	0.65	147	7.4	80	4.1	1.98	0.23	N2362	H, Z	1510	...	592	530	58
HD 57150	248.7798	–10.9117	3.85	0.72	39	2.5	27	2	0.93	0.22	...	...	...	...	...	289	52
HD 58343	231.0872	–00.2141	3.45	0.73	68	3.4	36	1.9	0.86	0.10	...	...	...	...	...	275	24
HD 58978	237.4106	–02.9978	2.30	0.70	66	3.3	35	1.8	0.84	0.10	...	...	...	...	...	270	23
HD 60325	230.4540	+02.5195	2.16	0.80	129	6.5	73	3.8	1.88	0.23	...	...	...	...	...	508	58
HD 60606	249.8536	–07.9482	2.56	0.49	158	8	87	4.5	2.18	0.26	...	...	...	...	...	575	65

Table 1. continued.

Name	l	b	π	σ_π	K	σ_K	H	σ_H	$N_{\rm Ca\,II}$	$\sigma_{N_{\rm Ca\,II}}$	as	as ref	D_H	D_{GS}	D_Z	$D_{\rm Ca\,II}$	$\sigma_{D_{\rm Ca\,II}}$
		mÅ		mÅ	10^{12} cm^{-2}				pc	pc	pc	pc	pc				
HD 61347	230.6031	+03.7951	1.97	1.0	467	24	307	15	9.65	1.45	...	...	...	...	...	2288	362
HD 61899	252.1281	–07.8163	2.92	0.49	190	10	110	6	2.91	0.39	...	...	...	...	...	743	97
HD 63005	242.4693	–00.9267	–1.13	1.2	275	14	191	10	6.60	1.16	PupOB1	H	2510	...	...	1588	282
HD 63462	242.2460	–00.2077	1.32	0.67	37	2	21	1.4	0.54	0.08	...	...	...	...	...	201	20
HD 66006	264.1985	–10.5053	3.89	6.13	60	4.2	45	3.6	1.82	0.57	...	...	...	...	...	494	132
HD 66546	268.3871	–12.4777	2.47	0.50	66	3.4	43	2.2	1.33	0.20	...	...	...	...	...	382	49
HD 67536	276.1126	–16.1399	2.61	0.46	46	2.3	25	1.3	0.62	0.07	...	...	...	...	...	218	17
HD 68273	262.8026	–07.6858	3.88	0.53	34	1.8	16	0.96	0.35	0.04	VelOB2	Z	...	...	410	157	10
HD 68450	254.4689	–02.0230	1.33	0.56	222	11	128	6.9	3.37	0.44	...	...	...	...	...	849	110
HD 68761	254.3713	–01.6188	1.50	0.58	250	13	137	7.4	3.41	0.42	...	...	...	...	...	858	107
HD 68980	253.5766	–00.8445	3.33	0.51	42	2.6	27	2.4	0.82	0.20	...	...	...	...	...	265	46
HD 69106	254.5175	–01.3306	0.92	0.61	206	11	107	7.3	2.52	0.36	...	...	...	...	...	655	88
HD 70930	264.9776	–06.4970	2.16	0.57	121	6.2	64	3.6	1.54	0.19	VelOB2	Z	...	...	410	429	46
HD 72067	262.0769	–03.0778	2.04	0.63	93	5	48	2.9	1.13	0.14	VelOB2	Z	...	...	410	335	35
HD 74455	266.6016	–03.6135	1.93	0.57	226	12	125	7	3.14	0.40	...	...	...	...	...	796	102
HD 75222	258.2892	+04.1768	1.97	0.7	364	19	233	12	7.03	1.05	...	...	...	...	...	1688	262
HD 76341	263.5348	+01.5210	0.82	0.62	92	4.7	56	2.9	1.58	0.22	...	...	...	...	...	438	53
HD 85871	279.4104	–00.8703	0.46	0.52	181	9.2	102	5.2	2.61	0.32	...	...	...	...	...	676	80
HD 85980	273.2544	+07.1374	3.86	0.63	33	1.7	17	0.91	0.40	0.05	...	...	...	...	...	168	11
HD 88661	283.0814	–01.4804	2.52	0.50	74	3.8	39	2.1	0.93	0.11	...	...	...	...	...	291	27
HD 89587	279.8352	+05.1930	0.60	0.60	242	12	122	6.2	2.80	0.30	...	...	...	...	...	719	77
HD 89688	241.0235	+46.2839	1.86	0.80	92	6.6	54	5.2	1.45	0.33	...	...	...	...	...	410	78
HD 91316	234.8870	+52.7674	0.57	0.82	82	4.3	45	2.5	1.12	0.14	...	...	...	...	...	334	34
HD 91452	288.3160	–05.1039	–1.08	0.67	333	18	225	13	7.40	1.34	...	...	...	...	...	1772	326
HD 92850	285.9842	+01.5422	0.79	0.74	356	18	218	12	6.18	0.90	...	...	...	...	...	1493	224
HD 92964	287.1091	–00.3583	0.48	0.52	513	26	271	14	6.50	0.74	CarOB1	H	2510	...	...	1565	193
HD 93130	287.5686	–00.8594	...	...	667	36	421	24	12.5	1.98	Col228	H	2510	...	...	2929	490
HD 93131	287.6681	–01.0822	0.50	0.54	437	22	280	14	8.46	1.23	...	...	...	...	...	2016	308
HD 93249	287.4069	–00.3592	...	...	435	23	287	16	9.07	1.52	Tr15	H	3720	...	...	2156	374
HD 93250	287.5066	–00.5423	0.29	0.59	841	42	609	31	22.8	4.29	Tr16	H	2630	...	...	5304	1043
HD 93403	287.5440	–00.3448	1.13	0.6	414	21	289	15	10.1	1.78	Tr16	H	2630	...	...	2385	434
HD 96248	289.9296	+00.2974	0.47	0.65	370	19	254	13	8.59	1.45	CarOB2	H	2000	...	...	2044	356
HD 96670	290.1973	+00.3969	0.82	0.73	380	19	275	14	10.3	1.93	CarOB2	H	2000	...	...	2434	469
HD 96715	290.2689	+00.3291	...	...	408	21	298	15	11.4	2.19	CarOB2	H	2000	...	...	2682	529
HD 96917	289.2842	+03.0588	–0.08	0.70	680	34	495	25	18.8	3.55	...	...	...	...	...	4373	863
HD 99264	296.3182	–10.5145	3.69	0.48	52	2.7	26	1.4	0.59	0.07	...	...	...	...	...	213	16
HD 99556	292.8663	+00.0875	2.10	0.55	119	6	68	3.5	1.77	0.22	...	...	...	...	...	483	55
HD 99872	296.6908	–10.6172	4.30	0.81	107	5.7	60	3.2	1.53	0.19	...	...	...	...	...	428	48
HD 100099	294.1366	–02.3379	0.02	0.75	363	18	236	12	7.29	1.09	CruOB1	H	2400	...	...	1748	273
HD 100444	294.3468	–02.0920	1.14	0.83	394	20	252	13	7.60	1.13	...	...	...	...	...	1817	281
HD 101131	294.7783	–01.6230	1.41	0.6	343	17	220	11	6.66	0.96	CruOB1	H	2400	...	...	1603	241
HD 101190	294.7816	–01.4904	–0.19	1.1	297	15	177	9.1	4.85	0.64	CruOB1	H	2400	...	...	1187	162
HD 101191	294.8399	–01.6755	...	...	350	18	217	11	6.26	0.87	CruOB1	H	2400	...	...	1511	219
HD 101205	294.8495	–01.6539	–1.44	1.42	377	19	238	12	7.04	1.00	CruOB1	H	2400	...	...	1690	252
HD 101223	294.8059	–01.4875	...	...	312	16	185	10	5.03	0.69	CruOB1	H	2400	...	...	1230	173

Table 1. continued.

Name	l	b	π	σ_π	K	σ_K	H	σ_H	$N_{Ca II}$	$\sigma_{N_{Ca II}}$	as	as ref	D_H	D_{GS}	D_Z	$D_{Ca II}$	$\sigma_{D_{Ca II}}$
		mÅ		mÅ	10^{12} cm^{-2}				pc	pc	pc	pc	pc				
HD 101298	294.9423	–01.6864	0.44	0.78	361	18	224	12	6.47	0.93	CruOB1	H	2400	...	...	1559	234
HD 101436	295.0394	–01.7096	–1.39	2.1	327	17	205	11	6.00	0.89	CruOB1	H	2400	...	...	1452	222
HD 101545	294.8771	–00.8091	1.16	1.1	337	17	220	11	6.84	1.03	CruOB1	H	2400	...	...	1644	255
HD 103884	296.7590	–00.2232	5.45	0.52	16	1.1	8	0.65	0.18	0.03	...	...	...	...	...	119	9
HD 104841	297.6439	–00.7787	4.33	0.53	124	6.4	41	2.2	0.72	0.06	...	...	...	...	...	242	15
HD 105056	298.9454	–07.0551	1.74	0.67	301	16	172	9.3	4.48	0.59	...	...	...	...	...	1103	148
HD 105435	295.9963	+11.5683	8.25	0.79	21	1.2	13	1	0.37	0.07	...	...	...	...	...	163	18
HD 105937	296.7837	+10.0277	9.53	0.73	6	0.66	4	0.63	0.13	0.06	...	...	...	...	...	107	15
HD 106343	298.9318	–01.8257	–0.16	0.55	358	18	190	9.6	4.58	0.51	...	...	...	...	...	1125	134
HD 109867	301.7113	–04.3511	0.03	0.55	290	15	141	7.3	3.14	0.33	...	...	...	...	...	796	86
HD 110432	301.9580	–00.2031	3.32	0.56	60	3.1	41	2.1	1.37	0.23	...	...	...	...	...	392	55
HD 112244	303.5527	+06.0305	1.73	0.57	225	11	133	6.8	3.61	0.46	...	...	...	...	...	903	117
HD 112272	303.4864	–01.4947	1.14	0.75	392	20	254	13	7.81	1.18	CenOB1	H	2510	...	...	1866	294
HD 113120	303.8675	–08.6251	2.07	0.68	74	4	35	1.9	0.76	0.08	...	...	...	...	...	252	20
HD 113904	304.6745	–02.4907	0.03	0.67	389	20	229	12	6.18	0.82	...	...	...	...	...	1492	207
HD 115363	305.8832	–00.9683	0.66	0.89	569	29	395	20	13.6	2.34	CenOB1	H	2510	...	...	3199	573
HD 115842	307.0804	+06.8343	0.0	0.78	280	14	193	9.7	6.57	1.10	...	...	...	...	...	1583	269
HD 116658	316.1123	+50.8446	12.44	0.86	6	0.41	3	1.9	0.07	0.08	...	...	...	...	...	93	20
HD 119159	309.9771	+05.3977	1.07	0.64	186	9.4	111	5.6	3.04	0.40	...	...	...	...	...	775	100
HD 122879	312.2630	+01.7905	–0.05	0.76	237	12	127	6.5	3.09	0.35	...	...	...	...	...	784	91
HD 125823	321.5656	+20.0226	7.79	0.76	81	4.2	32	1.8	0.62	0.06	U.CenLup	Z	...	...	140	218	14
HD 129116	325.9018	+20.0994	10.69	0.71	16	0.93	9	0.59	0.23	0.04	U.CenLup	Z	...	...	140	130	10
HD 133518	323.0822	+05.4606	3.21	0.75	104	5.4	31	1.8	0.52	0.04	...	...	...	...	...	197	11
HD 135160	319.6816	–02.8444	1.70	0.89	160	8	97	4.9	2.71	0.36	...	...	...	...	...	699	90
HD 136239	321.2281	–01.7448	0.65	1.01	674	34	438	22	13.5	2.02	...	...	...	...	...	3175	506
HD 141318	326.7903	–00.7335	0.89	0.89	114	6.1	73	4	2.20	0.35	...	...	...	...	...	582	84
HD 141637	346.0979	+21.7059	6.25	0.91	29	1.6	17	1.2	0.46	0.08	U.Sco	Z	...	...	145	182	18
HD 142096	350.7243	+25.3801	9.15	1.04	32	2	16	1.4	0.36	0.06	...	...	...	...	...	161	15
HD 142114	346.8768	+21.6134	7.52	1.18	15	0.97	8	0.98	0.19	0.05	U.Sco	Z	...	...	145	121	13
HD 142184	347.9325	+22.5452	8.30	1.18	37	2	20	1.3	0.49	0.07	U.Sco	Z	...	...	145	189	17
HD 142758	325.3065	–04.2765	–1.91	0.81	583	29	319	16	7.92	0.91	...	...	...	...	...	1892	239
HD 142883	350.8840	+24.0852	7.16	0.87	40	2.1	22	1.3	0.55	0.07	U.Sco	Z	...	...	145	203	17
HD 143118	338.7739	+11.0090	6.61	0.78	14	1	6	0.86	0.12	0.03	U.CenLup	Z	...	...	140	105	10
HD 143275	350.0969	+22.4904	8.12	0.88	38	2.1	23	1.4	0.64	0.10	ScoOB2	H	160	...	...	224	24
HD 143448	324.5485	–05.9714	0.79	0.74	119	8.8	66	3.5	1.66	0.23	...	...	...	...	...	458	55
HD 144217	353.1929	+23.5996	6.15	1.12	39	4	29	4.2	1.15	0.61	ScoOB2	H, Z	160	...	145	341	139
HD 144470	352.7497	+22.7730	7.70	0.87	39	2.1	21	1.3	0.51	0.07	U.Sco	Z	...	...	145	195	17
HD 145482	348.1166	+16.8354	6.97	0.79	10	0.71	5	0.56	0.11	0.02	U.Sco	Z	...	...	145	103	9
HD 145502	354.6087	+22.7002	7.47	1.11	62	3.1	41	2.1	1.30	0.20	U.Sco	Z	...	...	145	375	49
HD 147165	351.3130	+16.9989	4.44	0.81	62	3.2	28	1.6	0.59	0.06	U.Sco	Z	...	...	145	212	15
HD 147889	352.8573	+17.0436	7.36	1.19	52	3.5	35	2.5	1.14	0.25	...	...	...	...	...	339	60
HD 148184	357.9328	+20.6766	6.67	0.74	76	3.8	40	2.1	0.96	0.11	U.Sco	Z	...	...	145	296	27
HD 148379	337.2456	+01.5757	2.73	0.94	404	20	253	13	7.40	1.05	AraOB1a	H	1380	...	...	1772	264
HD 148546	343.3764	+07.1507	1.67	1.12	361	19	212	11	5.70	0.75	AraOB1a	H	1380	...	...	1383	190
HD 148605	353.0982	+15.7959	8.30	0.84	22	1.2	13	0.97	0.35	0.06	...	...	...	...	...	158	15
HD 148688	340.7197	+04.3474	0.38	0.88	353	18	202	10	5.27	0.64	...	...	...	...	...	1284	165

Table 1. continued.

Name	l	b	π	σ_π	K	σ_K	H	σ_H	N_{CaII}	$\sigma_{N_{CaII}}$	as	as ref	D_H	D_{GS}	D_Z	D_{CaII}	$\sigma_{D_{CaII}}$
		mÅ		mÅ	10^{12} cm^{-2}				pc	pc	pc	pc	pc				
HD 148937	336.3661	–00.2181	0.61	1.31	279	14	174	8.8	5.06	0.71	...	...	...	...	...	1236	177
HD 149038	339.3797	+02.5126	0.70	0.73	238	12	151	7.7	4.50	0.65	AraOB1a	H	1380	...	...	1108	162
HD 149404	340.5375	+03.0058	1.07	0.89	340	17	227	12	7.32	1.19	AraOB1a	H	1380	...	...	1753	293
HD 149711	340.3884	+02.3651	4.75	0.90	52	2.7	33	2	0.98	0.16	U.CenLup	Z	...	...	140	302	39
HD 149757	006.2812	+23.5877	7.12	0.71	45	2.4	25	1.6	0.63	0.09	...	...	...	...	...	222	22
HD 150135	336.7097	–01.5724	2.18	8.22	235	12	143	7.3	4.02	0.55	AraOB1a	H	1380	...	...	998	137
HD 150136	336.7117	–01.5743	–1.86	2.15	232	12	143	7.2	4.09	0.56	AraOB1a	H	1380	...	...	1014	141
HD 150168	336.0795	–02.2013	1.00	0.89	196	9.9	127	6.5	3.90	0.59	AraOB1a	H	1380	...	...	971	145
HD 150745	329.7706	–08.4789	3.89	0.77	98	5	64	3.3	1.99	0.31	...	...	...	...	...	533	74
HD 150898	329.9790	–08.4736	1.56	0.75	176	8.8	112	5.7	3.35	0.49	...	...	...	...	...	845	120
HD 151515	342.8119	+01.6984	0.55	0.81	644	33	432	22	14.0	2.26	ScoOB1	H	1910	...	...	3292	559
HD 151804	343.6156	+01.9379	0.48	0.83	438	22	280	14	8.43	1.22	ScoOB1	H	1910	...	...	2009	306
HD 152076	343.4154	+01.3957	...	...	444	23	261	14	7.03	0.94	ScoOB1	H	1910	...	...	1687	240
HD 152147	343.1535	+01.0964	...	...	409	22	246	13	6.81	0.94	ScoOB1	H	1910	...	...	1638	238
HD 152218	343.5304	+01.2778	...	...	392	20	251	13	7.58	1.13	ScoOB1	H	1910	...	...	1813	282
HD 152219	343.3927	+01.1836	...	...	390	20	236	12	6.59	0.89	ScoOB1	H	1910	...	...	1587	224
HD 152233	343.4776	+01.2209	...	...	448	22	277	14	7.96	1.09	ScoOB1	H	1910	...	...	1900	276
HD 152234	343.4628	+01.2155	0.55	1.2	438	22	269	14	7.66	1.07	ScoOB1	H	1910	...	...	1832	269
HD 152235	343.3111	+01.1041	–0.58	0.89	353	18	229	12	7.05	1.09	ScoOB1	H	1910	...	...	1693	269
HD 152236	343.0275	+00.8700	–1.13	0.90	397	20	238	12	6.57	0.86	ScoOB1	H	1910	...	...	1581	219
HD 152246	344.0339	+01.6656	–0.1	1.02	427	22	295	15	10.1	1.72	ScoOB1	H	1910	...	...	2388	422
HD 152247	343.6095	+01.2958	...	...	430	22	289	15	9.42	1.54	ScoOB1	H	1910	...	...	2235	380
HD 152248	343.4644	+01.1839	–1.37	1.43	465	23	298	15	9.01	1.31	ScoOB1	H	1910	...	...	2141	328
HD 152249	343.4488	+01.1649	...	...	455	23	287	14	8.48	1.18	ScoOB1	H	1910	...	...	2019	297
HD 152314	343.5227	+01.1435	...	...	430	22	327	16	13.7	2.86	ScoOB1	H	1910	...	...	3211	688
HD 152405	344.5646	+01.8920	–0.02	0.96	439	22	248	13	6.38	0.79	ScoOB1	H	1910	...	...	1538	204
HD 152408	344.0836	+01.4909	0.34	0.73	429	22	290	15	9.55	1.58	ScoOB1	H	1910	...	...	2264	388
HD 152424	343.3618	+00.8884	–0.15	0.86	392	20	229	12	6.12	0.80	ScoOB1	H	1910	...	...	1479	203
HD 152478	336.7830	–04.6360	4.34	0.82	66	3.4	37	2.1	0.94	0.12	...	...	...	...	...	293	30
HD 152590	344.8403	+01.8295	...	...	426	22	270	14	8.03	1.18	ScoOB1	H	1910	...	...	1917	296
HD 152667	344.5310	+01.4571	–0.86	0.84	391	20	258	13	8.16	1.26	ScoOB1	H	1910	...	...	1946	313
HD 152723	344.8110	+01.6052	1.20	1.46	461	23	288	15	8.39	1.20	ScoOB1	H	1910	...	...	2000	302
HD 153919	347.7544	+02.1735	–0.21	0.86	420	21	279	14	8.92	1.38	...	...	...	...	...	2120	343
HD 154090	350.8287	+04.2850	1.22	0.87	289	15	166	8.6	4.35	0.55	...	...	...	...	...	1073	140
HD 154368	349.9702	+03.2151	2.73	0.96	261	13	171	8.6	5.35	0.81	...	...	...	...	...	1302	200
HD 154445	019.2966	+22.9307	4.26	0.96	99	5	58	3.2	1.56	0.21	...	...	...	...	...	433	52
HD 154811	341.0616	–04.2191	2.38	0.94	331	17	213	11	6.48	0.97	...	...	...	...	...	1561	242
HD 154873	341.3454	–04.1096	1.46	1.24	249	12	149	7.5	4.10	0.53	...	...	...	...	...	1017	134
HD 155775	348.7967	+00.1456	0.08	0.80	240	12	150	8.1	4.37	0.64	...	...	...	...	...	1079	160
HD 155806	352.5858	+02.8683	0.73	0.77	251	13	150	7.6	4.12	0.54	...	...	...	...	...	1021	137
HD 156292	345.3498	-03.0846	0.69	1.01	432	23	271	14	7.94	1.16	...	...	...	...	...	1897	289
HD 156633	056.4049	+33.1367	3.77	0.56	57	3.5	34	2.7	0.93	0.18	...	...	...	...	...	291	43
HD 157038	349.9548	–00.7940	–1.15	0.78	714	36	517	26	19.4	3.62	...	...	...	...	...	4514	881
HD 157246	334.6447	–11.4786	2.87	0.75	57	3	28	1.7	0.63	0.08	...	...	...	...	...	221	18

Table 1. continued.

Name	l	b	π	σ_π	K	σ_K	H	σ_H	$N_{Ca II}$	$\sigma_{N_{Ca II}}$	as	as ref	D_H	D_{GS}	D_Z	$D_{Ca II}$	$\sigma_{D_{Ca II}}$
	mÅ		mÅ		10^{12} cm^{-2}				pc	pc	pc	pc	pc				
HD 157857	012.9706	+13.3103	2.76	1.15	336	18	232	15	7.93	1.63	...	...	...	...	...	1893	392
HD 159176	355.6666	+00.0493	0.96	1.59	248	12	149	7.7	4.12	0.55	...	...	...	...	...	1021	138
HD 160762	072.3219	+31.2650	6.58	0.56	102	5.5	51	2.7	1.16	0.13	...	...	...	...	...	343	32
HD 161056	018.6702	+11.5808	2.34	0.80	179	14	106	8.6	2.88	0.59	...	...	...	...	...	737	141
HD 162978	004.5367	+00.3012	–0.40	0.85	202	11	118	6.4	3.15	0.43	...	...	...	...	...	799	107
HD 163472	027.1570	+12.5536	3.93	0.97	110	6.1	71	4.5	2.17	0.39	...	...	...	...	...	574	94
HD 163800	007.0520	+00.6878	–0.18	0.97	182	9.1	122	6.1	3.96	0.62	SgrOB1	H	1580	...	...	984	153
HD 163892	007.1516	+00.6161	0.38	1.02	231	13	170	9.9	6.59	1.47	SgrOB1	H	1580	...	...	1587	350
HD 164284	030.9948	+13.3701	4.82	0.78	54	3	31	2	0.81	0.12	...	...	...	...	...	263	29
HD 164794	006.0089	–01.2050	0.66	1.01	233	12	139	7.1	3.81	0.50	SgrOB1	H	1580	...	...	950	127
HD 164816	006.0591	–01.1960	...	...	181	9.5	115	6.7	3.43	0.56	SgrOB1	H	1580	...	...	864	136
HD 164852	046.8314	+19.8070	3.17	0.71	194	11	97	6.6	2.21	0.30	...	...	...	...	...	583	75
HD 165024	343.3304	–13.8187	3.22	0.71	89	4.6	50	2.7	1.28	0.16	...	...	...	...	...	370	40
HD 165052	006.1212	–01.4819	2.27	1.13	270	14	177	9.1	5.54	0.86	SgrOB1	H	1580	...	...	1346	213
HD 166182	047.4189	+18.4248	2.14	0.63	93	5	67	3.8	2.48	0.51	...	...	...	...	...	646	121
HD 166734	018.9198	+03.6280	–0.25	1.4	564	28	402	20	14.6	2.60	...	...	...	...	...	3418	635
HD 168075	016.9428	+00.8422	...	...	539	27	373	19	12.8	2.18	SerOB1	H	2190	...	...	3008	535
HD 168112	018.4388	+01.6228	–0.6	1.25	475	25	314	17	9.96	1.64	SerOB2	H	2000	...	...	2359	404
HD 168137	016.9680	+00.7632	5.02	2.75	583	30	426	23	16.3	3.29	SerOB1	H	2190	...	...	3804	793
HD 168183	016.8119	+00.6680	0.34	1.36	609	31	402	21	12.7	2.02	SerOB2	H	2000	...	...	2991	500
HD 170235	007.9523	–06.7282	1.01	0.97	219	11	153	7.8	5.34	0.93	...	...	...	...	...	1301	226
HD 171432	014.6220	–04.9826	1.69	1.05	437	22	248	13	6.41	0.80	...	...	...	...	...	1545	206
HD 175754	016.3921	–09.9152	–0.13	0.97	428	24	260	16	7.30	1.17	...	...	...	...	...	1748	288
HD 179406	028.2285	–08.3118	2.68	0.80	116	5.9	70	3.7	1.95	0.27	...	...	...	...	...	523	66
HD 180968	056.3582	+04.8532	1.70	0.63	102	5.5	69	4.2	2.27	0.43	...	...	...	...	...	598	103
HD 182568	062.9037	+06.6268	4.21	0.58	46	3.1	35	2.8	1.47	0.47	...	...	...	...	...	413	109
HD 184915	031.7709	–13.2866	2.24	0.81	176	9	105	5.5	2.88	0.39	...	...	...	...	...	737	97
HD 185859	056.6419	–01.0031	1.15	0.78	236	12	182	9.3	7.88	1.76	...	...	...	...	...	1883	420
HD 187459	068.8088	+03.8515	1.47	0.62	284	16	208	12	7.98	1.75	...	...	...	...	...	1906	417
HD 187811	059.7235	–02.0663	5.27	0.69	14	1.4	9	1.9	0.27	0.15	...	...	...	...	...	140	35
HD 188209	080.9929	+10.0916	0.22	0.48	232	13	149	8.8	4.52	0.77	...	...	...	...	...	1112	187
HD 190429	072.5852	+02.6136	0.03	1.02	537	31	340	25	10.1	2.00	CygOB3	GS	...	1740	...	2391	482
HD 190603	069.4863	+00.3895	0.24	0.56	354	18	260	13	10.0	1.94	...	...	...	...	...	2377	469
HD 191781	081.1842	+06.6071	1.19	1.05	412	33	230	19	5.84	1.13	...	...	...	...	...	1414	272
HD 193237	075.8268	+01.3194	0.52	0.50	304	15	217	20	7.90	2.31	...	...	...	...	...	1886	542
HD 193793	080.9303	+04.1771	0.62	0.62	549	48	364	41	11.6	3.80	...	...	...	...	...	2735	887
HD 194279	078.6779	+01.9865	0.08	0.63	588	34	353	23	9.76	1.61	CygOB9	H	1200	...	...	2312	397
HD 194280	077.2007	+00.9225	0.12	0.81	275	24	210	15	8.87	2.92	CygOB1	H	1820	...	...	2110	681
HD 194839	079.5172	+01.8727	–0.36	0.64	426	26	295	20	10.1	2.24	CygOB9	H	1200	...	...	2398	536
HD 195592	082.3557	+02.9571	0.92	0.62	378	37	225	25	6.15	1.71	...	...	...	...	...	1486	402
HD 198478	085.7535	+01.4900	1.45	0.55	255	13	176	20	6.01	1.99	CygOB7	H, GS	830	830	...	1453	465
HD 200120	088.0296	+00.9707	2.90	0.64	30	2.1	15	1.1	0.34	0.05	...	...	...	...	...	155	13
HD 201345	078.4363	–09.5444	0.61	0.77	236	13	148	9	4.34	0.72	...	...	...	...	...	1070	176
HD 202214	098.5202	+07.9852	0.36	0.67	240	12	147	7.6	4.17	0.57	...	...	...	...	...	1032	144
HD 202904	080.9767	–10.0526	3.62	0.56	44	2.7	27	2.2	0.77	0.16	...	...	...	...	...	253	37

Table 1. continued.

Name	l	b	π	σ_π	K	σ_K	H	σ_H	$N_{Ca II}$	$\sigma_{N_{Ca II}}$	as	as ref	D_H	D_{GS}	D_Z	$D_{Ca II}$	$\sigma_{D_{Ca II}}$
		mÅ		mÅ	10^{12} cm^{-2}				pc	pc	pc	pc	pc				
HD 203064	087.6101	–03.8411	–0.05	0.55	217	12	144	7.9	4.60	0.78	CygOB7	H, GS	830	830	...	1130	190
HD 203374	100.5129	+08.6223	–0.70	0.70	277	15	197	11	7.12	1.40	CepOB2	GS	...	950	...	1707	338
HD 203938	090.5579	–02.2344	0.27	0.82	154	8.7	113	7.2	4.35	1.03	CygOB7	H, GS	830	830	...	1075	243
HD 204827	099.1667	+05.5525	0.97	0.79	276	15	194	11	6.85	1.33	CepOB2	H, GS, Z	830	950	615	1646	321
HD 205139	100.5454	+06.6218	1.36	0.50	258	13	186	9.4	6.91	1.28	CepOB2	GS, Z	...	950	615	1659	311
HD 206165	102.2713	+07.2469	0.72	0.49	237	12	177	8.9	7.09	1.44	CepOB2	H, GS, Z	830	950	615	1702	345
HD 206267	099.2904	+03.7383	2.78	0.79	234	12	146	10	4.25	0.76	CepOB2	H, GS	830	950	...	1050	184
HD 207198	103.1363	+06.9949	1.62	0.48	303	16	224	12	8.77	1.83	CepOB2	H, GS, Z	830	950	615	2087	439
HD 207538	101.5990	+04.6727	0.30	0.62	240	12	184	9.4	7.85	1.72	CepOB2	H, GS	830	950	...	1876	410
HD 209481	102.0052	+02.1835	0.70	0.46	263	14	168	9.8	5.05	0.83	CepOB2	H, GS	830	950	...	1235	203
HD 209975	104.8706	+05.3906	0.60	0.49	242	13	171	9.5	6.10	1.18	CepOB2	H, GS	830	950	...	1474	284
HD 210839	103.8279	+02.6108	1.98	0.46	237	12	173	8.8	6.59	1.27	CepOB2	H, GS	830	950	...	1587	306
HD 213087	108.4991	+06.3878	1.29	0.55	258	14	190	11	7.38	1.62	...	...	...	...	...	1768	387
HD 214680	096.6509	–16.9833	3.08	0.62	164	9.3	89	5.6	2.19	0.31	LacOB1	H, GS, Z	600	500	368	579	76
HD 216200	100.0421	–15.4742	3.00	0.75	144	7.6	97	7.9	3.17	0.75	LacOB1	GS	...	500	...	804	177
HD 217086	110.2206	+02.7198	1.20	0.92	303	15	208	10	7.03	1.13	CepOB3	H, GS	870	720	...	1688	278
HD 219287	110.8071	–01.1851	0.07	0.94	699	37	474	27	15.7	2.82	CasOB2	H	2630	...	...	3670	688
HD 220116	111.2051	–02.5101	1.87	0.99	243	20	189	17	8.37	3.29	...	...	...	...	...	1995	764
HD 223924	115.0468	–05.1639	0.65	1.04	226	17	106	16	2.29	0.63	...	...	...	...	...	602	147
HD 224572	115.5545	–06.3640	2.14	0.75	131	7.2	72	4.4	1.80	0.25	...	...	...	...	...	489	61
HD 303308	287.5936	–00.6131	...	...	1074	56	745	39	25.7	4.53	Tr16	H	2630	...	...	5957	1109
HD 306097	291.0649	–00.3763	...	...	326	17	217	12	6.96	1.18	CarOB2	H	2000	...	...	1672	288
HD 308813	294.7945	–01.6113	...	...	363	19	231	12	6.91	1.03	CruOB1	H	2400	...	...	1660	257
WR 110	010.8000	+00.3944	2.86	1.91	530	27	365	19	12.4	2.13	...	...	...	...	...	2920	523
WR 16	281.0798	–02.5509	–1.01	0.74	376	19	265	13	9.41	1.63	...	...	...	...	...	2232	398